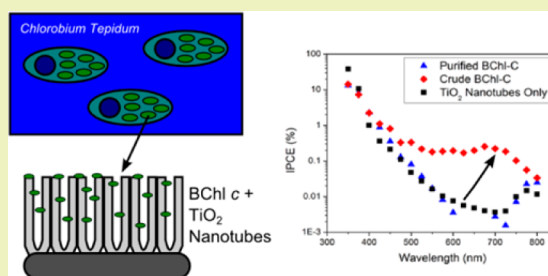


Visible Light Sensitization of TiO<sub>2</sub> Nanotubes by Bacteriochlorophyll-C Dyes for Photoelectrochemical Solar CellsLok-kun Tsui,<sup>†</sup> Justine Huang,<sup>‡</sup> Michal Sabat,<sup>†,§</sup> and Giovanni Zangari<sup>\*,†</sup><sup>†</sup>Department of Materials Science and Engineering, University of Virginia, 395 McCormick Rd., Charlottesville, Virginia 22904-4745, United States<sup>‡</sup>Department of Chemical Engineering, University of Virginia, 102 Engineers' Way, P.O. Box 400741, Charlottesville, Virginia 22904-4741, United States<sup>§</sup>Department of Chemistry, University of Virginia, McCormick Rd., P.O. Box 400319, Charlottesville, Virginia 22904-4319, United States

## S Supporting Information

**ABSTRACT:** Biomimetic sensitizers have evolved over millions of years to absorb and utilize sunlight and therefore are highly desirable to produce efficient, low cost, dye-sensitized photoelectrochemical solar cells. We report on the sensitization of TiO<sub>2</sub> nanotubes by bacteriochlorophyll-c (BChl *c*) extracted from photosynthetic bacteria. BChl *c* is notable for its high conversion efficiency inside the bacteria, which makes it a promising candidate for a naturally derived sensitizer for TiO<sub>2</sub>. A photocurrent conversion efficiency of 0.1% was observed at 600–800 nm, corresponding to the absorption peak in BChl *c*; a photoanode efficiency of 0.23% was measured at around  $-0.1 V_{SCE}$ . Stability tests under simulated sunlight showed stable photocurrents over the course of 14 min. Mechanisms that currently limit the efficiency include the formation of BChl *c* aggregates on TiO<sub>2</sub>, which may increase recombination, and possibly interface defects, which decrease charge injection to the nanotubes and trapping of photogenerated charges.

**KEYWORDS:** Biomimetic materials, TiO<sub>2</sub> nanotubes, Bacteriochlorophyll-c, Photoelectrochemistry, Dye-sensitized solar cells



## INTRODUCTION

The TiO<sub>2</sub> nanotube array system has been widely investigated as a photoanode material for photoelectrochemical cells (PECs) as well as dye-sensitized solar cells (DSSCs).<sup>1–7</sup> These nanotubes are formed from the anodization of Ti in electrolytes containing fluoride ions and exhibit 1-D charge transport along the length of the nanotube,<sup>8</sup> making them a more attractive and potentially more efficient system compared to nanoparticle TiO<sub>2</sub> where charges must hop randomly from particle to particle with reduced mobility.<sup>9,10</sup> The increased light scattering of TiO<sub>2</sub> nanotubes and the lower recombination rates have both been noted as advantages of TiO<sub>2</sub> NTs over nanoparticle TiO<sub>2</sub>.<sup>11</sup> Additionally, the long-term stability of TiO<sub>2</sub> nanotubes makes them technologically attractive for any photoelectrochemical application. However, the major drawback of TiO<sub>2</sub> is the large bandgap of anatase, 3.2 eV,<sup>12</sup> limiting the absorption to wavelengths below 378 nm and less than 10% of the solar radiation received.<sup>13</sup> As a consequence, the addition of dyes has been widely experimented with to extend the absorption of TiO<sub>2</sub> into the visible range. To date, the highest performing TiO<sub>2</sub>-based DSSC modified by metallorganic dyes is a Zn porphyrin-sensitized device coupled with a Co(II/III) redox shuttle that produced cell efficiencies of 12.3% under sunlight.<sup>14</sup> Recent developments of free-standing TiO<sub>2</sub> nanotubes transferred to transparent substrates have overcome challenges of a highly

resistive barrier layer and restriction of illumination direction, which has brought efficiencies up to 7.8% and made the nanotube system competitive with nanoparticle-based solar cells.<sup>15,16</sup>

There is a strong desire to develop inexpensive dyes for sensitization, and the natural chlorophyll structures found in biology are promising candidates for this application.<sup>17</sup> Chlorophylls extracted from spinach were used to sensitize TiO<sub>2</sub> and ZnO,<sup>18</sup> and a mixture of chlorophyll-a and chlorophyll-b extracted from spinach could be chemically processed to produce a Cu chlorophyll molecule that yielded up to 83% photon-to-current conversion efficiency at 400 nm, corresponding to an overall cell efficiency of 2.6%.<sup>19</sup> Exploiting the proton pumping mechanism of the photosensitive bacteriorhodopsin protein extracted from *Halobacterium salinarum*, Allam et al. achieved a current density of 0.65 mA/cm<sup>2</sup> photocurrent density for water splitting under AM 1.5 sunlight paired with 7 μm TiO<sub>2</sub> nanotubes.<sup>20</sup>

For photoelectrochemical applications, bacteriochlorophylls found in photosynthetic bacteria hold greater promise than their plant-derived counterparts.<sup>21</sup> Variants of these chlorophylls are differentiated by the chemical groups at the edges.<sup>22</sup> The

Received: June 18, 2014

Revised: July 22, 2014

Published: August 11, 2014

mechanism that enables these bacteria to more efficiently use light is the self-assembly of bacteriochlorophyll molecules into structures that boost the absorption of photons, enabling the bacteria to run photosynthesis with a photon flux as low as one photon per 8 h.<sup>23,24</sup> Upon illumination, the bacteriochlorophyll is placed in an excited state, which is followed by transfer of charge to neighboring molecules for photosynthesis.<sup>25,26</sup> If the photogenerated electrons were injected into TiO<sub>2</sub> instead, this could potentially result in a highly efficient solar cell that would use these bacteriochlorophylls as sensitizers. The LUMO (−3.2 eV) and HOMO (−5.2 eV) levels of an aggregated mixture of BChl types including *c* indicate that these energy levels bracket the conduction band edge of TiO<sub>2</sub> (−4.2 eV),<sup>21,27</sup> which provides a driving force for electron injection into TiO<sub>2</sub> in a similar manner as the Ru-based N-719 dye used in DSSCs with a HOMO of −5.45 eV and a LUMO of −3.85 eV.<sup>28</sup> Frigaard measured the absorption spectra in solution of various chloro- and bacteriochlorophylls and detected strong peaks at 364–469 and 654–795 nm.<sup>29</sup> Miyatake and Tamiaki characterized the absorption spectra of the bacteriochlorophyll-*c* (BChl *c*) and found a sharp absorption peak located at 740 nm for aggregates and 667 nm for the monomeric form, along with a broad absorption peak at 440 nm contributed by carotenoids.<sup>22</sup> Lu et al. have demonstrated a photoelectric response on mesoporous WO<sub>3</sub>/TiO<sub>2</sub> films using a mixture of purple nonsulfur bacteria photosynthetic reaction centers.<sup>26</sup>

While bacteriochlorophyll-based photoelectrochemical systems have been proposed, they have not been used as dyes on TiO<sub>2</sub> nanotubes before. We report on the synthesis of BChl *c*-modified TiO<sub>2</sub> nanotubes, demonstrating the generation of photocurrent under visible light illumination and stable operation over 14 min under simulated sunlight. Slow photocurrent transients are observed under visible light, indicating losses due to trapping of photogenerated electrons within the BChl *c*. We find crude BChl *c* to be more effective than purified BChl *c*, suggesting that the purification process may denature the product or that it could somewhat hinder the attachment of these molecules to the TiO<sub>2</sub> nanotubes.

## EXPERIMENTAL SECTION

TiO<sub>2</sub> nanotubes were synthesized by anodizing Ti foils (99%, annealed, metals basis, Alfa Aesar) that were cut into 2 cm × 0.7 cm × 0.127 cm sections. Prior to anodization they were degreased by sonication in acetone, isopropanol, and methanol. Anodization was carried out in a solution of 0.5 wt % NH<sub>4</sub>F (99.99%, metals basis, Sigma-Aldrich) and 11 vol % H<sub>2</sub>O (DI Millipore) in ethylene glycol (99.8% Sigma-Aldrich) at 20 V for 1 h.<sup>30</sup> In order to verify whether the TiO<sub>2</sub> nanotubes high surface area may effectively enhance the photocurrent, planar TiO<sub>2</sub> was used as a benchmark; the latter was synthesized by anodizing in 0.5 M H<sub>2</sub>SO<sub>4</sub> at 20 V for 30 minutes, producing a flat oxide film. Anodization was controlled with a Kepco BOP-100 using LabVIEW connected to Ti foil as the anode and a Pt mesh as the cathode. Samples were annealed at 350 °C for 3 h in air in order to obtain the anatase TiO<sub>2</sub> phase.<sup>31</sup>

Adsorption of BChl *c* at the TiO<sub>2</sub> nanotube surface was carried by soaking TiO<sub>2</sub> nanotube samples for 1–7 days (see the Supporting Information for BChl *c* bacteria production, extraction, and absorption spectroscopy procedures). The morphology of the adsorbed aggregates was examined by using a field emission-scanning electron microscope (FE-SEM, JEOL 6700F). Photocurrent measurements were carried out in a solution of 0.2 M Na<sub>2</sub>SO<sub>4</sub> and 0.1 M NaCH<sub>3</sub>COO (pH 7) in a three electrode configuration with a saturated calomel reference electrode (SCE) and a platinum mesh as the counter electrode. Monochromated light measurements between 350 and 800 nm were collected to identify the range of wavelengths where the addition of BChl *c* resulted in photocurrent generation. The illumination came from a Princeton

TS428 tungsten/halogen lamp and SP1250 monochromator combination with a UV filter used at all wavelengths above 500 nm. The power density of the light as a function of wavelength was measured by a Newport Model 1931-C power meter with 0.35 cm radius detector, which was then used to calculate incident photocurrent efficiency (IPCE)<sup>32</sup> as a function of wavelength.

$$\text{IPCE}(\lambda) = \text{electrons cm}^{-2} \text{ s}^{-1}(\lambda) / \text{photons cm}^{-2} \text{ s}^{-1}(\lambda)$$

The integrated incident intensity was 68 mW/cm<sup>2</sup>. Monochromatic light measurements were controlled by a CHI-920C potentiostat at a fixed bias of 0.3 V<sub>SCE</sub>. Photocurrent measurements were also taken under AM 1.5 simulated sunlight with an Oriel Sol 1A light source.

## RESULTS AND DISCUSSION

Figure 1 compares the morphology of bare TiO<sub>2</sub> nanotubes (a) with those modified by adsorption of crude bacteriochlorophyll

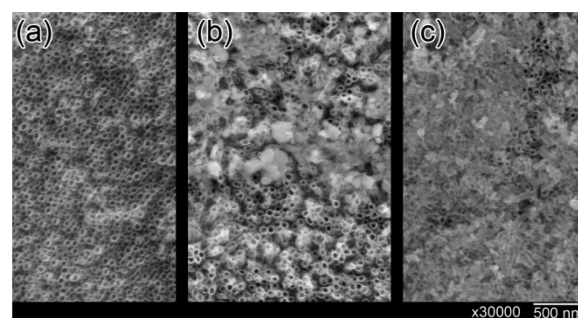


**Figure 1.** Surface morphology of BChl *c* modified TiO<sub>2</sub> nanotubes (a) no deposited material, (b) 1 day of soaking, and (c) 4 days of soaking.

for 1 day (b) or 4 days (c). Only the samples modified with crude BChl *c* were analyzed because no change in color was observed when the purified material was added on the TiO<sub>2</sub> nanotubes. BChl *c* aggregates are seen to form at random sites, eventually covering the entire surface. The precise character of these aggregates is difficult to evaluate due to the pronounced topography of the TiO<sub>2</sub> nanotube surface; others however have observed on flat surfaces the formation of self-assembled cyclic structures.<sup>33</sup> The increase in aggregate size with longer adsorption time would eventually lead to thickening of the BChl *c* layer as well as to the photogeneration of charge carriers at locations farther from the TiO<sub>2</sub>/BChl *c* interface, possibly hindering charge collection and causing recombination. We have observed similar effects with TiO<sub>2</sub> nanotubes modified by Cu<sub>2</sub>O and Fe<sub>2</sub>O<sub>3</sub> inorganic sensitizers.<sup>34</sup>

The incident photon-to-current conversion efficiency (IPCE) is reported as a function of wavelength in Figure 2(a). For unmodified TiO<sub>2</sub> nanotubes, the photocurrent efficiency drops to below 10<sup>−3</sup> % beyond 500 nm. Little change is observed in the UV portion of the spectrum after BChl *c* modification; however, efficiency on the order of 0.1% is observed in the wavelength range centered between 600 and 800 nm. This absorption peak coincides with the absorption peak for BChl *c* (Figure S1, Supporting Information) as reported both by Frigaard<sup>29</sup> and Miyatake and Tamiaki.<sup>22</sup> As more BChl *c* is being adsorbed with increased deposition time, the photocurrent efficiencies at all wavelengths are indeed observed to decrease. Next, the behavior of purified BChl *c* is compared with the crude material in Figure 2(b). We find that purified BChl *c* provides no enhancement in the photocurrent as a function of wavelength, and the IPCE spectrum in Figure 2(b) is indistinguishable from that of the unmodified TiO<sub>2</sub> nanotubes. In Figure 2(c), the photocurrent

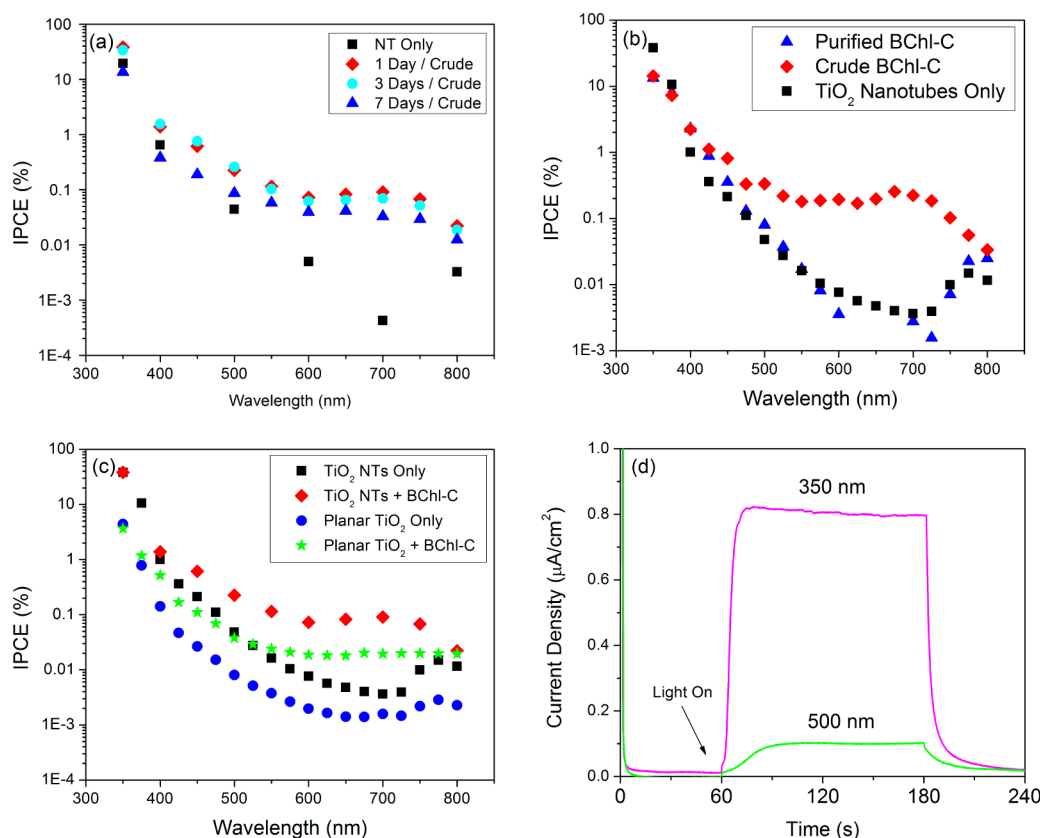


**Figure 2.** Photocurrent measurements on TiO<sub>2</sub> nanotubes and TiO<sub>2</sub> nanotubes modified by BChl *c*. (a) Effect of adsorption time shows that an optimal soaking time is 1 day, and further coverage decreases photocurrent efficiency. (b) IPCE from crude BChl *c* is compared with that of purified BChl *c*; visible light absorption is only seen in the crude material. (c) Performance of TiO<sub>2</sub> nanotubes is compared with that of planar TiO<sub>2</sub>, showing an enhancement likely due to the high surface area. (d) Photocurrent transients for 350 and 500 nm illumination are compared. The slow onset under 500 nm illumination is associated with trap-filling behavior when visible light is absorbed by BChl *c* aggregates.

efficiency of the planar TiO<sub>2</sub> films is compared with that of TiO<sub>2</sub> nanotubes to verify that the higher surface area morphology of the nanotubes indeed contributes to enhance efficiency; the enhancement observed is on the order of 5–10 times. Finally, the photocurrent transients in the UV at 350 nm and in the visible at 500 nm are shown in Figure 2(d). While a sharp onset is observed for the response under UV light, corresponding primarily to photocurrent generation from TiO<sub>2</sub> nanotubes, the response in the visible range at 500 nm has a slow onset transient. A slow onset response is characteristic of the accumulation of photogenerated charges in trap states,<sup>35,36</sup> which suggests the presence of defects in the BChl *c* aggregates associated with disorganized molecular assemblies. The addition of the linker 3-mercaptopropionic acid has been shown to improve adhesion of bacteriorhodopsin to TiO<sub>2</sub> nanotubes and suggests that the attachment of BChl *c* may be similarly enhanced.<sup>20</sup>

The performance and stability of the TiO<sub>2</sub> nanotubes modified by 2 days of soaking in BChl *c* were tested under simulated sunlight. A linear sweep voltammetry LSV (Figure 3(a)) was collected under simulated sunlight from about  $-0.5$  to  $+0.6$  V<sub>SCE</sub>. The photoanode efficiency under applied bias (Figure 3(b)) was calculated using the expression

$$\eta = J_{\text{pc}}(E_{\text{OER}} - E_{\text{applied}})/P$$

where  $J_{\text{pc}}$  is the photocurrent density,  $E_{\text{OER}}$  is the potential of the oxygen evolution reaction at pH 7 ( $E_{\text{OER}} = 1.23$  V<sub>SHE</sub> - 0.059 pH = 0.576 V<sub>SCE</sub>), and  $P$  is the power density of simulated sunlight

(100 mW/cm<sup>2</sup>). Photoanode efficiencies reach a maximum of 0.05% for the unmodified TiO<sub>2</sub> nanotubes and 0.23% for the BChl *c* modified TiO<sub>2</sub> nanotubes. A major challenge of narrow bandgap inorganic semiconductors, such as Cu<sub>2</sub>O, for TiO<sub>2</sub> sensitization is their tendency to rapidly degrade under illumination, on the order of only minutes.<sup>37,38</sup> While in the bacteria, the BChl are contained in chlorosomes that protect against degradation;<sup>39</sup> studies involving the use of BChl *a* as sensitizers for medical phototreatment or fluorescence imaging raise concerns about potential instabilities due to oxidation during illumination. This limitation may necessitate the development of more stable derivatives by substituting the central metal atom with Pd.<sup>40,41</sup> Therefore, it is important to establish if similar instabilities may occur for photoelectrochemical applications. Figure 3(c) shows the photocurrent transients for both TiO<sub>2</sub> nanotubes, which are known to be stable, and TiO<sub>2</sub> nanotubes modified with BChl *c*. A 60 s delay in the dark is permitted in order to allow the dark current to establish a steady state value. As TiO<sub>2</sub> itself is stable, the measurement for the nanotubes was only held for 120 s to establish a baseline photocurrent as a comparison before turning the light off. For the BChl *c* modified TiO<sub>2</sub> nanotubes, after an initial spike associated with equilibration to surface recombination,<sup>42</sup> the photocurrent transients reach a steady state with no sign of decay over the course of 14 min. This indicates that under these operating conditions, the BChl *c* modification is stable. Longer tests are needed to establish the stability of BChl *c* on time scales on the



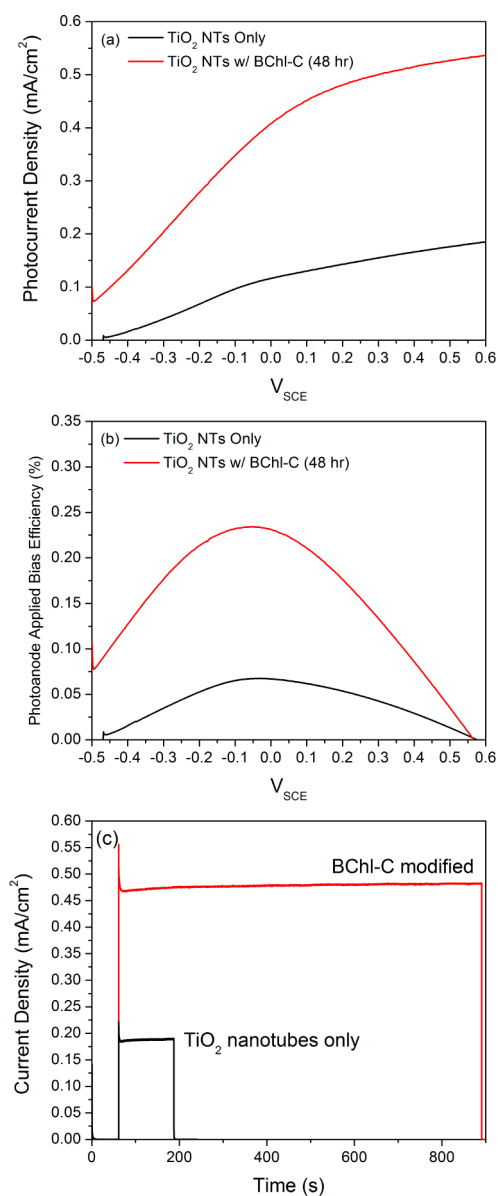


**Figure 3.** (a) LSV of TiO<sub>2</sub> nanotubes and BChl *c* modified TiO<sub>2</sub> nanotubes, (b) calculated photoanode efficiency of TiO<sub>2</sub> nanotubes as a function of potential, and (c) stability of TiO<sub>2</sub>/BChl *c* photoanodes tested under simulated sunlight, showing no losses in photocurrent over the course of 14 min.

order of hours and days, which are more representative of the actual operating conditions of a photoelectrochemical solar cell.

These results serve as a first proof of concept that BChl *c* can be used as a visible light sensitizer when paired with TiO<sub>2</sub> nanotubes. Visible light photogenerated charge carriers in the BChl *c* aggregates can in fact be injected in TiO<sub>2</sub>, and the stability of the configuration appears satisfactory. The main drawback is that the photocurrent efficiencies in the visible light range are below 1%. It is important to understand the origin of such low efficiency, specifically whether this may be due to the aggregation of BChl *c*, hindering charge collection, or low injection probability due to interface defects or perhaps electronic effects. The interface between the nanotubes and the BChl *c* is a likely source of charge trapping; the slow onset transients under visible light illumination in fact point to this as an area where the photocurrent conversion efficiencies may be improved. Both

issues could be tackled by promoting the adsorption of mono- or multilayer adsorption of ordered BChl *c* assemblies, enabling control of the amount of BChl *c* deposited and fostering reproducible contacts at the interface. The molecular organization of the sensitizers has shown to be essential for exciton transport.<sup>43</sup> Functionalization of BChl *c* molecules to form mono- or multilayers on TiO<sub>2</sub> is therefore likely to strongly enhance their performance.

In summary, TiO<sub>2</sub> nanotubes have been successfully sensitized by BChl *c*. Photocurrent measurements under monochromatic light have demonstrated a photon-to-current conversion efficiency of 0.1% in the window of 600–800 nm, which coincides with the observed absorption peaks in the BChl *c* absorption spectra. BChl *c* aggregates were observed by SEM, their size increasing with longer adsorption time; this aggregation, coupled with strong trapping of photogenerated charges, resulted in a limited photocurrent efficiency. The better performance of the crude material indicates the lack of a need for purification, which potentially would reduce the complexity of fabrication of similar devices. The stability of BChl *c*/TiO<sub>2</sub> was tested under simulated sunlight, and the photocurrents were observed to be stable at least over the course of 14 min.

## ■ ASSOCIATED CONTENT

### Supporting Information

Procedures for growing the bacteria precursors, extracting bacteriochlorophyll-*c*, and taking UV–vis spectra, along with the absorption spectrum obtained on BChl *c*. This material is available free of charge via the Internet at <http://pubs.acs.org>.

## ■ AUTHOR INFORMATION

### Corresponding Author

\*Tel.: +1 434-243-5474. Fax: +1 434-982-5660. E-mail: [gz3e@virginia.edu](mailto:gz3e@virginia.edu).

### Notes

The authors declare no competing financial interest.

## ■ ACKNOWLEDGMENTS

We gratefully acknowledge the support of the ARCS foundation. Preparation of BChl *c* on TiO<sub>2</sub> and its characterization by UV–vis spectroscopy was performed in collaboration with Prof. Anthony Spano (Department of Biology, University of Virginia).

## ■ REFERENCES

- (1) Ahn, B.-E.; Kim, H. S.; Yang, S. K.; Ahn, K.-S.; Kang, S. H. Double layered nanoarchitecture based on anodic TiO<sub>2</sub> nanotubes for dye-sensitized solar cells. *J. Photochem. Photobiol., A* **2014**, *274*, 20–26.
- (2) Ghicov, A.; Albu, S. P.; Hahn, R.; Kim, D.; Stergiopoulos, T.; Kunze, J.; Schiller, C.-A.; Falaras, P.; Schmuki, P. TiO<sub>2</sub> nanotubes in dye-sensitized solar cells: critical factors for the conversion efficiency. *Chem.—Asian J.* **2009**, *4*, 520–525.
- (3) Roy, P.; Albu, S. P.; Schmuki, P. TiO<sub>2</sub> nanotubes in dye-sensitized solar cells: Higher efficiencies by well-defined tube tops. *Electrochem. Commun.* **2010**, *12*, 949–951.
- (4) Zhong, P.; Que, W.; Liao, Y.; Zhang, J.; Hu, X. Improved performance in dye-sensitized solar cells by rationally tailoring anodic TiO<sub>2</sub> nanotube length. *J. Alloy. Compd.* **2012**, *540*, 159–164.
- (5) Wu, H. P.; Li, L. L.; Chen, C. C.; Diao, E. W. G. Anodic TiO<sub>2</sub> nanotube arrays for dye-sensitized solar cells characterized by electrochemical impedance spectroscopy. *Ceram. Int.* **2012**, *38*, 6253–6266.
- (6) Zhu, K.; Vinzant, T. B.; Neale, N. R.; Frank, A. J. Removing structural disorder from oriented TiO<sub>2</sub> nanotube arrays: reducing the

dimensionality of transport and recombination in dye-sensitized solar cells. *Nano Lett.* **2007**, *7*, 3739–3746.

(7) Jennings, J. R.; Ghicov, A.; Peter, L. M.; Schmuki, P.; Walker, A. B. Dye-sensitized solar cells based on oriented TiO<sub>2</sub> nanotube arrays: transport, trapping, and transfer of electrons. *J. Am. Chem. Soc.* **2008**, *130*, 13364–13372.

(8) Roy, P.; Berger, S.; Schmuki, P. TiO<sub>2</sub> nanotubes: Synthesis and applications. *Angew. Chem., Int. Ed. Eng.* **2011**, *50*, 2904–2938.

(9) Roy, P.; Kim, D.; Lee, K.; Spiecker, E.; Schmuki, P. TiO<sub>2</sub> nanotubes and their application in dye-sensitized solar cells. *Nanoscale* **2010**, *2*, 45–59.

(10) De Jongh, P. E.; Vanmaekelbergh, D. Trap-limited electronic transport in assemblies of nanometer-size TiO<sub>2</sub> particles. *Phys. Rev. Lett.* **1996**, *77*, 3427–3430.

(11) Zhu, K.; Neale, N. R.; Miedaner, A.; Frank, A. J. Enhanced charge-collection efficiencies and light scattering in dye-sensitized solar cells using oriented TiO<sub>2</sub> nanotubes arrays. *Nano Lett.* **2007**, *7*, 69–74.

(12) Kavan, L.; Grätzel, M.; Gilbert, S. E.; Klemenz, C.; Scheel, H. J. Electrochemical and photoelectrochemical investigation of single-crystal anatase. *J. Am. Chem. Soc.* **1996**, *118*, 6716–6723.

(13) Linsebigler, A. L.; Lu, G.; Yates, J. T. Photocatalysis on TiO<sub>2</sub> surfaces: Principles, mechanisms, and selected results. *Chem. Rev.* **1995**, *95*, 735–758.

(14) Yella, A.; Lee, H.-W.; Tsao, H. N.; Yi, C.; Chandiran, A. K.; Nazeeruddin, M. K.; Diao, E. W.-G.; Yeh, C.-Y.; Zakeeruddin, S. M.; Grätzel, M. Porphyrin-sensitized solar cells with cobalt (II/III)-based redox electrolyte exceed 12% efficiency. *Science* **2011**, *334*, 629–634.

(15) Kim, J. Y.; Noh, J. H.; Zhu, K.; Halverson, A. F.; Neale, N. R.; Park, S.; Hong, K. S.; Frank, A. J. General strategy for fabricating transparent TiO<sub>2</sub> nanotube arrays for dye-sensitized photoelectrodes: Illumination geometry and transport properties. *ACS Nano* **2011**, *5*, 2647–2656.

(16) Lin, J.; Guo, M.; Yip, C. T.; Lu, W.; Zhang, G.; Liu, X.; Zhou, L.; Chen, X.; Huang, H. High temperature crystallization of free-standing anatase TiO<sub>2</sub> nanotube membranes for high efficiency dye-sensitized solar cells. *Adv. Funct. Mater.* **2013**, *23*, 5952–5960.

(17) McHale, J. L. Hierarchical light-harvesting aggregates and their potential for solar energy applications. *J. Phys. Chem. Lett.* **2012**, *3*, 587–597.

(18) Amao, Y.; Yamada, Y. Near-IR light-sensitized voltaic conversion system using nanocrystalline TiO<sub>2</sub> film by Zn chlorophyll derivative aggregate. *Langmuir* **2005**, *21*, 3008–3012.

(19) Kay, A.; Grätzel, M. Artificial photosynthesis. 1. Photosensitization of titania solar cells with chlorophyll derivatives and related natural porphyrins. *J. Phys. Chem.* **1993**, *97*, 6272–6277.

(20) Allam, N. K.; Yen, C.-W.; Near, R. D.; El-Sayed, M. A. Bacteriorhodopsin/TiO<sub>2</sub> nanotube arrays hybrid system for enhanced photoelectrochemical water splitting. *Energy Environ. Sci.* **2011**, *4*, 2909–2914.

(21) Marek, P. L.; Hahn, H.; Balaban, T. S. On the way to biomimetic dye aggregate solar cells. *Energy Environ. Sci.* **2011**, *4*, 2366–2378.

(22) Miyatake, T.; Tamiaki, H. Self-aggregates of natural chlorophylls and their synthetic analogues in aqueous media for making light-harvesting systems. *Coord. Chem. Rev.* **2010**, *254*, 2593–2602.

(23) Blankenship, R. E. Identification of a key step in the biosynthetic pathway of bacteriochlorophyll c and its implications for other known and unknown green sulfur bacteria. *J. Bacteriol.* **2004**, *186*, 5187–5188.

(24) Egawa, A.; Fujiwara, T.; Mizoguchi, T.; Kakitani, Y.; Koyama, Y.; Akutsu, H. Structure of the light-harvesting bacteriochlorophyll c assembly in chlorosomes from *Chlorobium limicola* determined by solid-state NMR. *Proc. Natl. Acad. Sci. U.S.A.* **2007**, *104*, 790–795.

(25) Xu, H.; Zhang, R.-B.; Ma, S.-H.; Qu, Z.-W.; Zhang, X.-K.; Zhang, Q.-Y. Theoretical studies on the mechanism of primary electron transfer in the photosynthetic reaction center of *Rhodobacter sphaeroides*. *Photosynth. Res.* **2002**, *74*, 11–36.

(26) Lu, Y.; Yuan, M.; Liu, Y.; Tu, B.; Xu, C.; Liu, B.; Zhao, D.; Kong, J. Photoelectric performance of bacteria photosynthetic proteins entrapped on tailored mesoporous WO<sub>3</sub>-TiO<sub>2</sub> films. *Langmuir* **2005**, *21*, 4071–4076.

(27) Orendorz, A.; Wusten, J.; Ziegler, C.; Gnaser, H. Photoelectron spectroscopy of nanocrystalline anatase TiO<sub>2</sub> films. *Appl. Surf. Sci.* **2005**, *252*, 85–88.

(28) Lenzmann, F.; Krueger, J.; Burnside, S.; Brooks, K.; Grätzel, M.; Gal, D.; Rühle, S.; Cahen, D. Surface photovoltage spectroscopy of dye-sensitized solar cells with TiO<sub>2</sub>, Nb<sub>2</sub>O<sub>5</sub>, and SrTiO<sub>3</sub> nanocrystalline photoanodes: Indication for electron injection from higher excited dye states. *J. Phys. Chem. B* **2001**, *105*, 6347–6352.

(29) Frigaard, N.-U.; Larsen, K. L.; Cox, R. P. Spectrochromatography of photosynthetic pigments as a fingerprinting technique for microbial phototrophs. *FEMS Microbiol. Ecol.* **1996**, *20*, 69–77.

(30) Tsui, L.-k.; Homma, T.; Zangari, G. Photocurrent conversion in anodized TiO<sub>2</sub> nanotube arrays: effect of the water content in anodizing solutions. *J. Phys. Chem. C* **2013**, *117*, 6979–6989.

(31) Tighineanu, A.; Ruff, T.; Albu, S. P.; Hahn, R.; Schmuki, P. Conductivity of TiO<sub>2</sub> nanotubes: Influence of annealing time and temperature. *Chem. Phys. Lett.* **2010**, *494*, 260–263.

(32) Chen, Z.; Jaramillo, T. F.; Deutsch, T. G.; Kleiman-Shwarsstein, A.; Forman, A. J.; Gaillard, N.; Garland, R.; Takane, K.; Heske, C.; Sunkara, M. Accelerating materials development for photoelectrochemical hydrogen production: Standards for methods, definitions, and reporting protocols. *J. Mater. Res.* **2010**, *25*, 3–16.

(33) De Feyter, S.; De Schryver, F. Two-dimensional dye assemblies on surfaces studied by scanning tunneling microscopy. *Top. Curr. Chem.* **2005**, *258*, 205–255.

(34) Tsui, L.-k.; Zangari, G. The influence of morphology of electrodeposited Cu<sub>2</sub>O and Fe<sub>2</sub>O<sub>3</sub> on the conversion efficiency of TiO<sub>2</sub> nanotube photoelectrochemical solar cells. *Electrochim. Acta* **2013**, *100*, 220–225.

(35) Solbrand, A.; Henningsson, A.; Södergren, S.; Lindström, H.; Hagfeldt, A.; Lindquist, S. Charge transport properties in dye-sensitized nanostructured TiO<sub>2</sub> thin film electrodes studied by photoinduced current transients. *J. Phys. Chem. B* **1999**, *103*, 1078–1083.

(36) Schwarzbürg, K.; Willig, F. Influence of trap filling on photocurrent transients in polycrystalline TiO<sub>2</sub>. *Appl. Phys. Lett.* **1991**, *58*, 2520–2522.

(37) Wu, L.; Tsui, L.-k.; Swami, N.; Zangari, G. Photoelectrochemical stability of electrodeposited Cu<sub>2</sub>O films. *J. Phys. Chem. C* **2010**, *114*, 11551–11556.

(38) Tsui, L.-k.; Zangari, G. Modification of TiO<sub>2</sub> nanotubes by Cu<sub>2</sub>O for photoelectrochemical, photocatalytic, and photovoltaic devices. *Electrochim. Acta* **2014**, *128*, 341–348.

(39) Ganapathy, S.; Oostergetel, G. T.; Wawrzyniak, P. K.; Reus, M.; Gomez Maqueo Chew, A.; Buda, F.; Boekema, E. J.; Bryant, D. A.; Holzwarth, A. R.; de Groot, H. J. M. Alternating syn-anti bacteriochlorophylls form concentric helical nanotubes in chlorosomes. *Proc. Natl. Acad. Sci. U.S.A.* **2009**, *106*, 8525–8530.

(40) Dandler, J.; Wilhelm, B.; Scheer, H. Photochemistry of bacteriochlorophylls in human blood plasma: 1. Pigment stability and light-induced modifications of lipoproteins. *Photochem. Photobiol.* **2010**, *86*, 331–341.

(41) Cao, W.; Ng, K. K.; Corbin, I.; Zhang, Z.; Ding, L.; Chen, J.; Zheng, G. Synthesis and evaluation of a stable bacteriochlorophyll-analog and its incorporation into high-density lipoprotein nanoparticles for tumor imaging. *Bioconjugate Chem.* **2009**, *20*, 2023–2031.

(42) Peter, L. M. Dynamic aspects of semiconductor photoelectrochemistry. *Chem. Rev.* **1990**, *90*, 753–769.

(43) Huijser, A.; Marek, P. L.; Savenije, T. J.; Siebbeles, L. D. A.; Scherer, T.; Hauschild, R.; Szymkowski, J.; Kalt, H.; Hahn, H.; Balaban, T. S. Photosensitization of TiO<sub>2</sub> and SnO<sub>2</sub> by artificial self-assembling mimics of the natural chlorosomal bacteriochlorophylls. *J. Phys. Chem. C* **2007**, *111*, 11726–11733.